#### ORIGINAL ARTICLE



# The Effect of Posterior Lumbar Interbody Fusion in Lumbar Spine Stenosis with Diffuse Idiopathic Skeletal Hyperostosis: A Finite Element Analysis

Norihiro Nishida<sup>1</sup>, Muzammil Mumtaz<sup>2</sup>, Sudharshan Tripathi<sup>2</sup>, Yogesh Kumaran<sup>2</sup>, Amey Kelkar<sup>2</sup>, Takashi Sakai<sup>1</sup>, Vijay K. Goel<sup>2</sup>

- OBJECTIVE: Lumbar spinal canal stenosis (LSS) with diffuse idiopathic skeletal hyperostosis (DISH) can require revision surgery because of the intervertebral instability after decompression. However, there is a lack of mechanical analyses for decompression procedures for LSS with DISH.
- METHODS: This study used a validated, threedimensional finite element model of an L1-L5 lumbar spine, L1-L4 DISH, pelvis, and femurs to compare the biomechanical parameters (range of motion [ROM], intervertebral disc, hip joint, and instrumentation stresses) with an L5-sacrum (L5-S) and L4-S posterior lumbar interbody fusion (PLIF). A pure moment with a compressive follower load was applied to these models.
- RESULTS: ROM of L5-S and L4-S PLIF models decreased by more than 50% at L4-L5, respectively, and decreased by more than 15% at L1-S compared with the DISH model in all motions. The L4-L5 nucleus stress of the L5-S PLIF increased by more than 14% compared with the DISH model. In all motions, the hip stress of DISH, L5-S, and L4-S PLIF had very small differences. The sacroiliac joint stress of L5-S and L4-S PLIF models decreased by more than 15% compared with the DISH model. The stress values of the screws and rods in the L4-S PLIF model was higher than in the L5-S PLIF model.

■ CONCLUSIONS: The concentration of stress because of DISH may influence adjacent segment disease on the nonunited segment of PLIF. A shorter-level lumbar interbody fixation is recommended to preserve ROM; however, it should be used with caution because it could provoke adjacent segment disease.

#### **INTRODUCTION**

n diffuse idiopathic skeletal hyperostosis (DISH), the connective tissues of the spinal region, especially the anterior longitudinal ligament (ALL), reduce flexibility because of continuous ossification and concentrates stress on the caudal or cranial intervertebral disc and vertebrae in discontinuous ossification.1,2 DISH is highly prevalent in the lumbar spine of older patients rather than younger patients.<sup>3,4</sup> Lumbar spinal canal stenosis (LSS) is also a common disease in elderly patients, which presents with low back pain, leg pain, and cauda equina syndrome. In LSS, conservative treatment may be effective, although when symptoms do not improve, it is often followed by surgical treatment through a posterior lumbar interbody fusion (PLIF), which provides widespread spinal canal decompression and intervertebral stability.<sup>5,6</sup> In some patients with DISH, LSS may occur simultaneously, which has been reported to be a risk factor for surgical treatment of LSS.<sup>7,8</sup>

# Key words

- Diffuse idiopathic skeletal hyperostosis (DISH)
- Finite element analysis
- Lumbar spine stenosis (LSS)
- Posterior lumbar interbody fusion (PLIF)
- Stress

# **Abbreviations and Acronyms**

3D: Three-dimensional

**ALL**: Anterior longitudinal ligament

ASD: Adjacent segment disease

CT: Computed tomography

DISH: Diffuse idiopathic skeletal hyperostosis

LSS: Lumbar spinal canal stenosis
PEEK: Polyetheretherketone
PLIF: Posterior lumbar interbody fusion

FE: Finite element

it should be used with caution because it could provoke adjacent segment disease.

ROM: Range of motion SIJ: Sacroiliac joint

From the <sup>1</sup>Department of Orthopedic Surgery, Yamaguchi University Graduate School of Medicine, Ube City, Yamaguchi Prefecture, Japan; and <sup>2</sup>Engineering Center for Orthopaedic Research Excellence (E-CORE), Departments of Bioengineering and Orthopaedics, The University of Toledo, Toledo, Ohio, USA

To whom correspondence should be addressed: Norihiro Nishida, M.D., Ph.D.

[E-mail: nishida3@yamaguchi-u.ac.jp]

Citation: World Neurosurg. (2023) 176:e371-e379. https://doi.org/10.1016/j.wneu.2023.05.063

Journal homepage: www.journals.elsevier.com/world-neurosurgery

Available online: www.sciencedirect.com

1878-8750/\$ - see front matter © 2023 Elsevier Inc. All rights reserved.

Nakajima et al.<sup>7</sup> reported that LSS with DISH required revision surgery at higher rates because of the intervertebral instability after decompression with or without fusion. Kato et al.9 reported that PLIF in patients with LSS and DISH had an increased risk for cage retropulsion. Some studies reported that the cause of the retropulsion was the concentration of stress from the long lever arm and continuous ossification, which can influence the intervertebral space of the nonunited segment, leading to adjacent segment disease (ASD).10 When clinicians encounter LSS with DISH, it is difficult to determine whether they should conduct longer length fixation to reduce ASD or operate on only the responsible intervertebral level to preserve the range of motion (ROM) in the lumbar. The current study explores the biomechanical effect of LSS with DISH and PLIF and examines the stress distribution on the instrumentation, sacroiliac joint (SIJ), hip joint, intervertebral disc, and interbody cage in a patient with DISH and subsequent LSS with PLIF fixation. A three-dimensional (3D) finite element (FE) L1-L5 lumbar, pelvic, and femur model was used to examine how stresses and mobility change in a model containing a L1-L4 DISH with an L4-S PLIF.

#### **METHODS**

#### FE Model of L1-L5 Lumbar, Pelvis, and Femurs

A previously developed and validated FE lumbar spine, pelvis, and femoral model" was used for this study. The geometry of the model was generated from a computed tomography (CT) image of a 55-year-old woman with lumbar spine, pelvis, and the hip joints without any abnormalities, degeneration, or deformation. All procedures performed in studies involving human participants were in accordance with the ethical standards of the institutional and/or national research committee. Necessary approvals for use of these images were obtained from the institutional review board and ethics committee at the authors' institution. The 3D geometry of the lumbar spine model was built using MIMICS software (Materialise, Leuven, Belgium). For geometry smoothing, Geomagic studio software (Raindrop Geomagic Inc., Research Triangle Park, North Carolina, USA) was used. Spine discs were meshed using IAFEMESH software (University of Iowa, Iowa, USA) while the vertebrae and pelvis was meshed using Hypermesh software (Altair Engineering Inc., Troy, Michigan, USA). The thickness of the cortical bone for the vertebrae and pelvis was 1 mm surrounding the cancellous bone. After developing the FE model geometry, all meshed regions were assembled in ABAQUS software (Dassault Systems, Simulia Inc., Providence, Rhode Island, USA). The cortical bone of the vertebrae and spinal discs was assigned as linear hexahedral elements, whereas the cancellous bone of both vertebrae and pelvis was assigned with tetrahedral

Truss elements were used for the ligamentous tissues. The spinopelvic FE model consists of the ALL, posterior longitudinal ligament, interspinous ligament, supraspinous ligament, capsular ligament, and ligamentum flavum in the lumbar spine. The model also includes the anterior sacroiliac ligament, interspinous ligament, long posterior sacroiliac ligament, short posterior sacroiliac ligament, sacrospinous ligament, and sacrotuberous ligament

pelvis ligament. The SIJs, spine facets, articular cartilages, and pubic symphysis were modeled as nonlinear soft contacts.

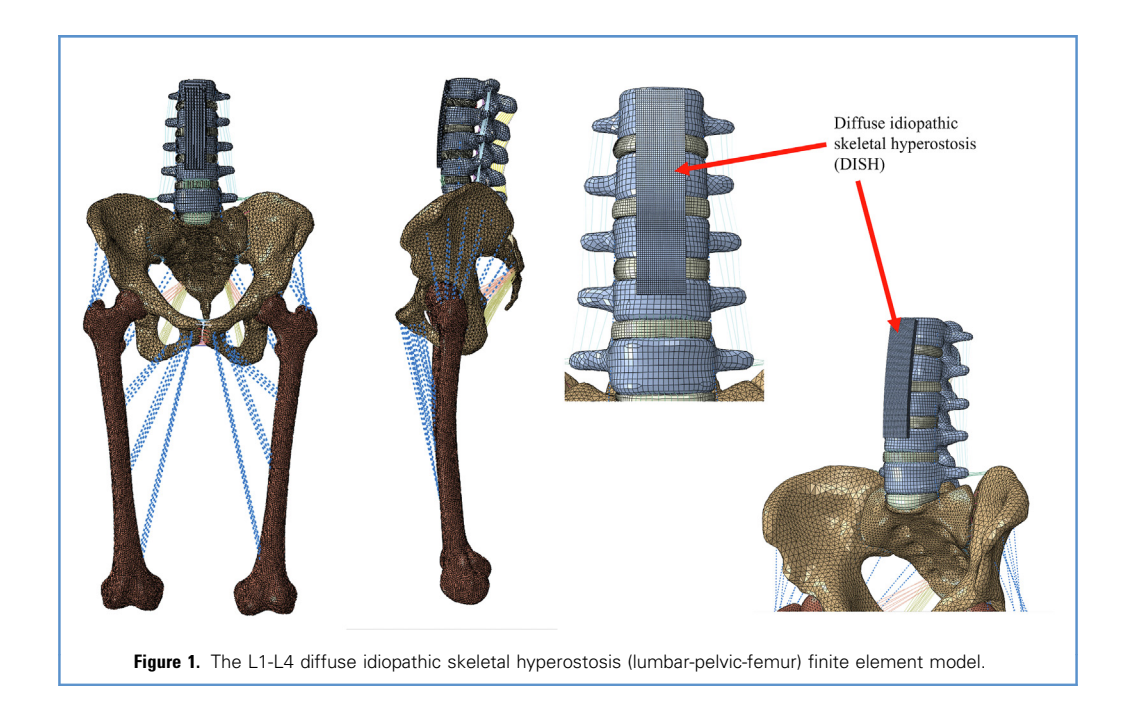
The femur was positioned relative to the pelvis according to a study conducted by Wu et al. 12 by first defining the anatomic planes of each femur based on femoral bony features and the hip joint center of rotation and, then, aligning these defined planes with the anatomic planes of the pelvis. Hip joint functionality was validated against research conducted by Anderson et al.13 and Harris et al.14 The experimental study simulated motions, specifically walking, ascending stairs, and descending stairs,13 described in an earlier instrumented hip clinical study by Bergmann et al. 15 This study validated hip functionality by comparing hip contact stress and area against those determined by Anderson et al. 13 (described earlier) and Harris et al. 14 Harris et al. 14 developed patient-specific FE models based on volunteer scans but the relative positions of the femoral heads and acetabula of these models were driven per data from Bergmann et al. 15; contact metrics produced by the models were measured and reported. The same boundary conditions and activities were simulated in the current work: the pelvis was constrained while the femur was positioned per the Bergmann angles corresponding to walking, ascending stairs, and descending stairs<sup>15</sup> (Figure 1). This model was considered as the intact model with no disease or instrumentation. Spinopelvic parameters in this model included the sacral slope, lumbar lordosis, pelvic incidence, and pelvic tilt. The sacral slope, lumbar lordosis, pelvic incidence, and pelvic tilt of this model were  $26^{\circ}$ ,  $42^{\circ}$ ,  $45^{\circ}$ , and  $11^{\circ}$ , respectively.

**Material Properties.** The material properties of all the structures in the FE model were used from previous studies for cortical and cancellous bones, annulus, nucleus, ligaments, and joints are summarized in **Table 1**. <sup>16-19,22</sup> Specifically, muscles spanning the hip joint from their physiologic origins to insertions were included as connector elements with stiffnesses assigned per Phillips et al. (**Table 1**). <sup>23-25</sup>

**DISH Model.** The LI-L4 DISH model was constructed by removing the LI-L4 ALL and by placing a 5-mm plate with the same mechanical properties as cortical bone, anterior to the LI-L4 vertebral body. The contact used among DISH, the intervertebral disc, and the vertebral body was defined using the TIE constraint in ABA-QUS. This DISH model was assembled in ABAQUS 6.14, and the final model contained 222,753 nodes and 780,522 elements.

**PLIF Model.** The L5-S PLIF model was constructed by removing a part of both L5 lamina, part of both facet joints, the ligamentum flavum, part of the annulus fibrosus, and the nucleus pulposus. Four pedicle screws were placed in the L5 and S1 vertebrae, and bilateral rods were used for fixation. Two 23-mm-long polyetheretherketone (PEEK) interbody cages were inserted into the L5-S1 intervertebral space without the nucleus pulposus (**Figure 2A**).

The L4-S PLIF model was constructed by removing a part of both L4 lamina, part of both facet joints, all ligamentum flavum, part of the annulus fibrosus, and all of the nucleus pulposus for sufficient insertion of the cage. Six pedicle screws were placed in the L4, L5, and S1 vertebrae, and bilateral rods were used for fixation. Two 23-mm-long PEEK interbody cages were inserted



into the L4-L5 and L5-S1, respectively, into the intervertebral space without the nucleus pulposus (Figure 2B). Screws and PEEK interbody cages were rigidly fixed using the TIE constraint in ABAQUS, and solid fusion was assumed between the cage and vertebral bodies.

The pedicle screws, rods, and PEEK interbody cage material properties were obtained from the literature<sup>26</sup> (Table 1).

Loading and Boundary Conditions. A 400N compressive follower load was applied tangentially to each vertebra of the spine using wire elements to simulate the effect of muscle forces and the weight of the upper trunk. A pure moment of 7.5 Nm was applied to the superior surface of LI to simulate physiologic loading; loading was applied in flexion, extension, left and right lateral bending, and left and right axial rotation. To constrain the models, the femurs were fixed in all degrees of freedom to prevent relative displacement of the legs in a 2-leg stance condition. 19,22

#### **DATA ANALYSIS**

After the generation of each model, an FE analysis of the spine and pelvis was performed in ABAQUS 6.14. The ROM, intradiscal (nucleus) stresses, left—right average hip stress (MPa), and left—right average SIJ stress (MPa) were calculated for the DISH, L5-S PLIF, and L4-S PLIF models. The maximum von Mises stress was noted for the nucleus stresses, hip stress, and SIJ stresses. The maximum von Mises stresses across the cages, rods, and screws were analyzed.

The percentage change (%) was calculated using the following equation:

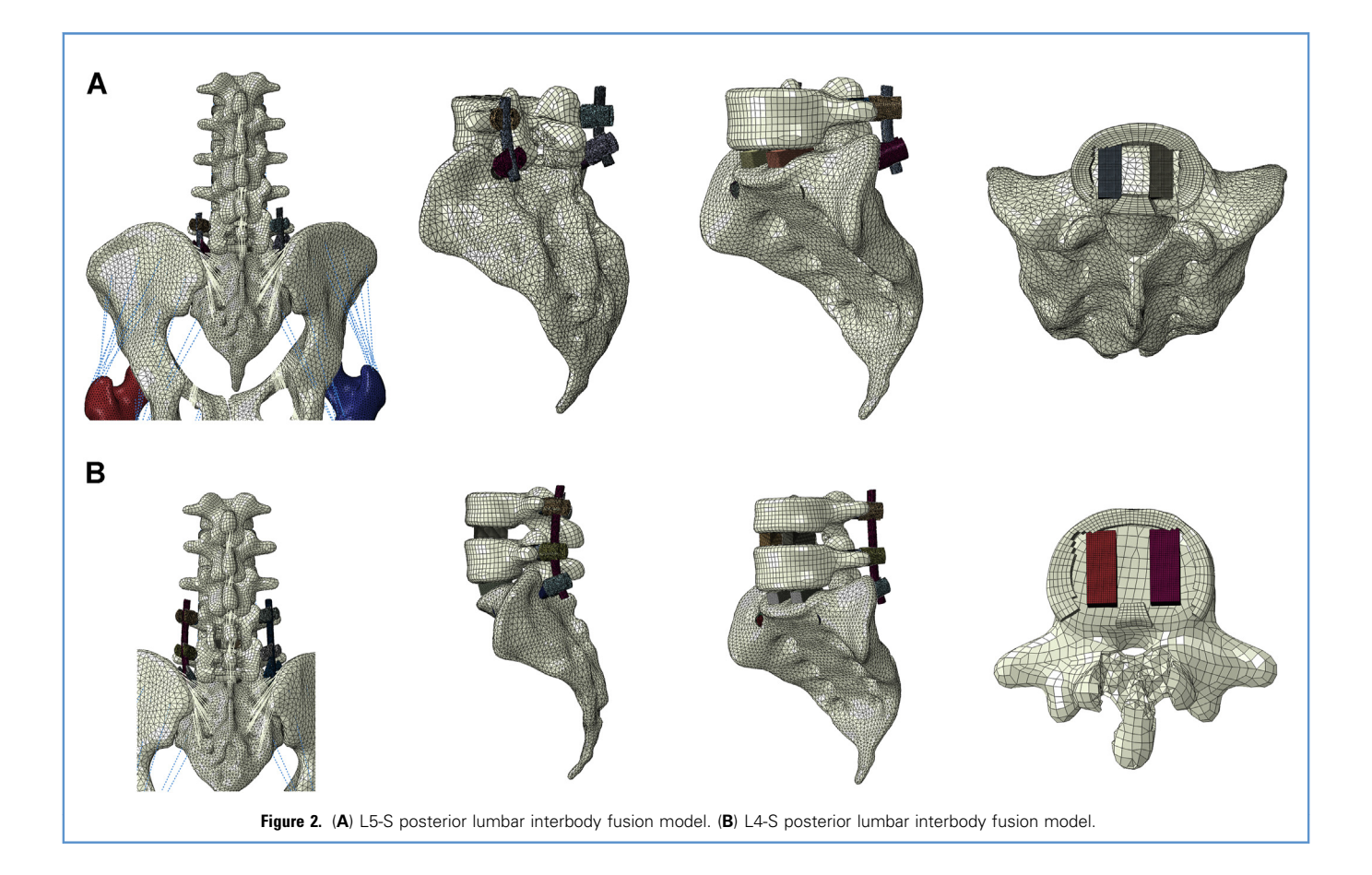
$$Percentage \ change \ (\%) = \frac{PLIF \ Model \ Data - DISH \ Model \ Data}{Intact \ Model \ Data} \star_{\textbf{IOO}}$$

#### **RESULTS**

### **ROM**

In extension, ROM of the L5-S PLIF and L4-S PLIF models decreased by 83% and 97% at L4-L5, respectively, and decreased by 37% and 40%, respectively, at L1-S compared with DISH model. In flexion, ROM of the L5-S PLIF models increased by 123% at L4-L5 and decreased by 13% at L1-S compared with the DISH model. ROM of the L4-S PLIF models decreased by 76% at L4-L5 and 50% at LI-S compared with the DISH model. In left bending, ROM of the L5-S PLIF models increased by 55% at L4-L5 compared with the DISH model. ROM of the L4-S PLIF models decreased by 86% at L4-L5 and 77% at L1-S compared with the DISH model. In right bending, ROM of the L5-S PLIF models increased by 25% at L4-L5 compared with the DISH model. ROM of the L4-S PLIF models decreased by 90% at L4-L5 and 75% at L1-S compared with the DISH model. In left rotation, ROM of the L5-S PLIF models increased by 1036% at L4-L5 and decreased by 16% at L1-S compared with the DISH model. ROM of the L4-S PLIF models decreased by 24% at L4-L5 and 45% at L1-S compared with the DISH model. In right rotation, ROM of the L5-S PLIF models increased by 973% at L4-L5 and 16% at L1-S compared with the DISH model. ROM of the L4-S PLIF models decreased by 16% at L4-L5 and 49% at L1-S compared with the DISH model. In all motions, ROM of the L4-L5 PLIF and L5-S PLIF models at L5-S

Table 1. Material Properties Assigned to the Finite Element Model <sup>2,16-19</sup>					
Component	Material Properties	Constitutive Relation	Element Type		
Vertebral cortical bone	$E=$ 12 000 MPa $\upsilon=$ 0.3	• •			
Vertebral cancellous bone	E = 100  MPa $\upsilon = 0.2$	Isotropic, elastic	4 nodes tetrahedral element (C3D4		
Pelvic cortical bone (sacrum, ilium)	$E = 17\ 000\ \text{MPa}$ $\upsilon = 0.3$	Isotropic, elastic	4 nodes tetrahedral element (C3D4		
Sacrum cancellous bone	Heterogeneous	Isotropic, elastic	4 nodes tetrahedral element (C3D4		
llium cancellous bone	$E=70$ MPa Isotropic, elast $\upsilon=0.2$		4 nodes tetrahedral element (C3D4)		
Femur cortical bone	E = 17 000  MPa v = 0.29	Isotropic, elastic	4 nodes tetrahedral element (C3D4		
Femur cancellous bone	E = 100  MPa $\upsilon = 0.2$	Isotropic, elastic	4 nodes tetrahedral element (C3D4		
Ground substance of annulus fibrosis	$C_{10} = 0.035$ $K_1 = 0.296$ $K_2 = 65$	Hyperelastic anisotropic (HGO)	8 nodes brick element (C3D8)		
Nucleus pulposus	E = 1  MPa v = 0.499	Isotropic, elastic	8 nodes brick element (C3D8)		
Anterior longitudinal	7.8 MPa (<12%), 20 MPa (>12%)	Nonlinear hypoelastic	Truss element (T3D2)		
Posterior longitudinal	10 MPa (<11%), 20 MPa (>11%)	Nonlinear hypoelastic	Truss element (T3D2)		
Ligamentum flavum	15 MPa (<6.2%), 19.5 MPa (>6.2%)	Nonlinear hypoelastic	Truss element (T3D2)		
Intertransverse	10 MPa (<18%), 58.7 MPa (>18%)	Nonlinear hypoelastic	Truss element (T3D2)		
Interspinous	10 MPa (<14%), 11.6 MPa (>14%)	Nonlinear hypoelastic	Truss element (T3D2)		
Supraspinous	8 MPa (<20%), 15 MPa (>20%)	Nonlinear hypoelastic	Truss element (T3D2)		
Capsular	7.5 MPa (<25%), 32.9 MPa (>25%)	Nonlinear hypoelastic	Truss element (T3D2)		
Anterior SIJ <sup>20</sup>	125 MPa (5%), 325 MPa (>10%), 316 MPa (>15%)	Nonlinear hypoelastic	Truss element (T3D2)		
Short posterior SI	43 MPa (5%), 113 MPa (>10%), 110 MPa (>15%)	Nonlinear hypoelastic	Truss element (T3D2)		
Long posterior SI	150 MPa (5%), 391 MPa (>10%), 381 MPa (>15%)	Nonlinear hypoelastic	Truss element (T3D2)		
Intraosseus	40 MPa (5%), 105 MPa (>10%), 102 MPa (>15%)	Nonlinear hypoelastic	Truss element (T3D2)		
Sacrospinous	304 MPa (5%), 792 MPa (>10%), 771 MPa (>15%)	Nonlinear hypoelastic	Truss element (T3D2)		
Sacrotuberous	326 MPa (5%), 848 MPa (>10%), 826 MPa (>15%)	Nonlinear hypoelastic	Truss element (T3D2)		
Gluteus maximus	k = 344 N/mm	_	Connector element		
Gluteus medius	k = 779 N/mm	_	Connector element		
Gluteus minimus	k = 660 N/mm	_	Connector element		
Psoas major <sup>21</sup>	k = 100 N/mm	_	Connector element		
Adductor magnus	k = 257 N/mm	_	Connector element		
Adductor longus	k = 134 N/mm	_	Connector element		
Adductor brevis	k = 499 N/mm	_	Connector element		
Polyetheretherketone (interbody cage)	E = 3500  MPa v = 0.3	Isotropic, elastic	Hexahedral elements		
Titanium (rods)	E = 120000  MPa $\upsilon = 0.3$	Isotropic, elastic	Hexahedral elements		
Pedicle screws (titanium-alloy)	E = 110000  MPa v = 0.3	Isotropic, elastic	Hexahedral elements		



decreased by more than 60% compared with the DISH model (Figure 3).

#### **Nucleus Stresses**

In extension, the L4-L5 nucleus stress of L5-S PLIF increased by 14% compared with the DISH model. In flexion, the L4-L5 nucleus stress of L5-S PLIF increased by 54% compared with the DISH model. In left bending, the L4-L5 nucleus stress of L5-S PLIF increased by 25% compared with the DISH model. In right bending, the L4-L5 nucleus stress of L5-S PLIF increased by 27% compared with the DISH model. In left rotation, the L4-L5 nucleus stress of L5-S PLIF increased by 13% compared with the DISH model. In right rotation, the L4-L5 nucleus stress of L5-S PLIF increased by 18% compared with the DISH model (Figure 4).

# **Left—Right Average hip Stress**

In all motions, the left—right average hip stress of DISH, L5-S PLIF, and L4-S PLIF had very small differences (0%—3%).

### Left-Right Average SIJ Stress

In extension, the left—right average SIJ stress of the L5-S PLIF and L4-S PLIF models decreased by 17% and 19%, respectively, compared with the DISH model. In flexion, the left—right average SIJ stress of the L5-S PLIF and L4-S PLIF models decreased by 17%

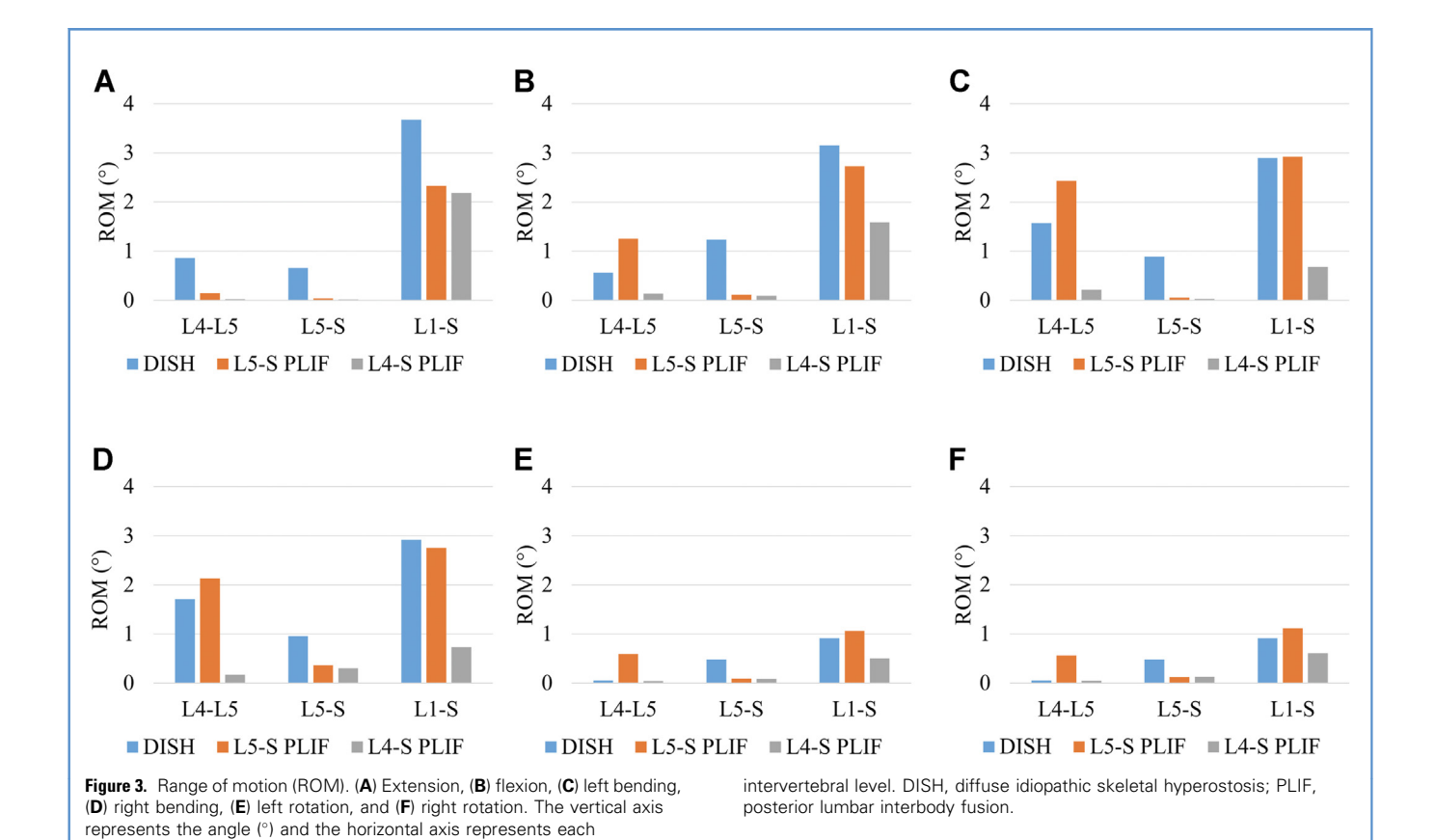
and 16%, respectively, compared with the DISH model. In left bending, the left—right average SIJ stress of the L5-S PLIF and L4-S PLIF models decreased by 15% and 16%, respectively, compared with the DISH model. In right bending, the left—right average SIJ stress of the L5-S PLIF and L4-S PLIF models decreased by 18% and 18%, respectively, compared with the DISH model. In left rotation, the left—right average SIJ stress of the L5-S PLIF and L4-S PLIF model decreased by 16% and 17%, respectively, compared with the DISH model. In right rotation, the left—right average SIJ stress of the L5-S PLIF and L4-S PLIF model decreased by 17% and 18%, respectively, compared with the DISH model (Figure 5).

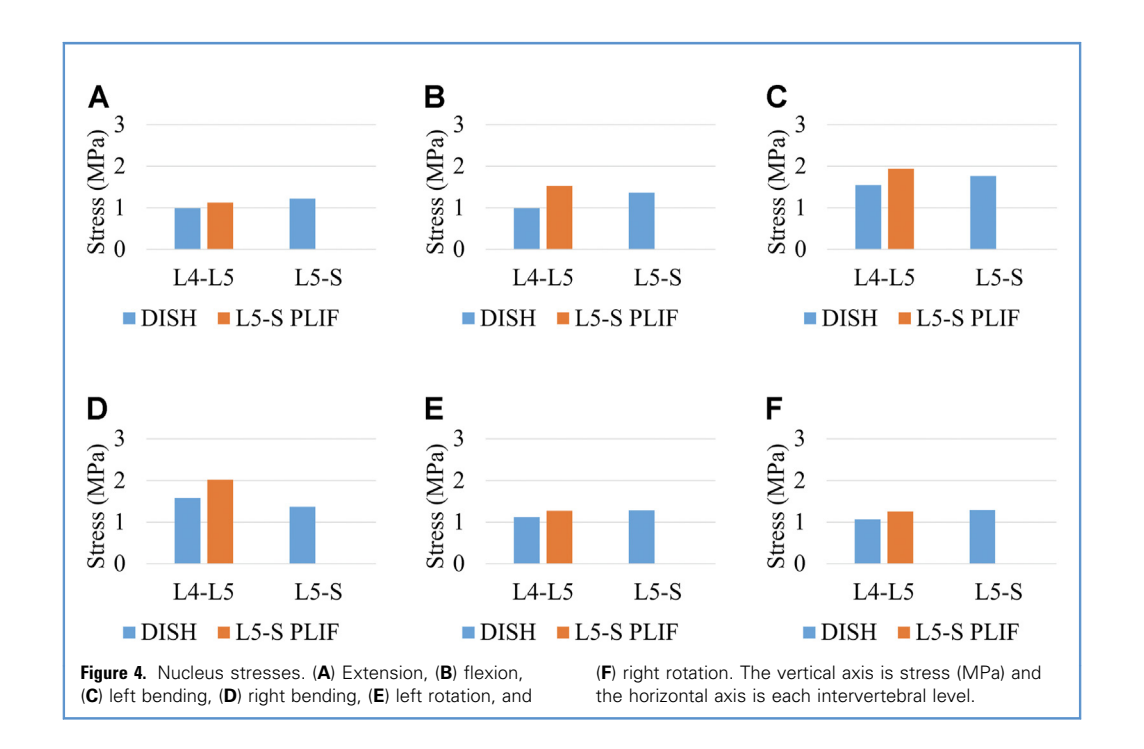
## **Stress on the Implants**

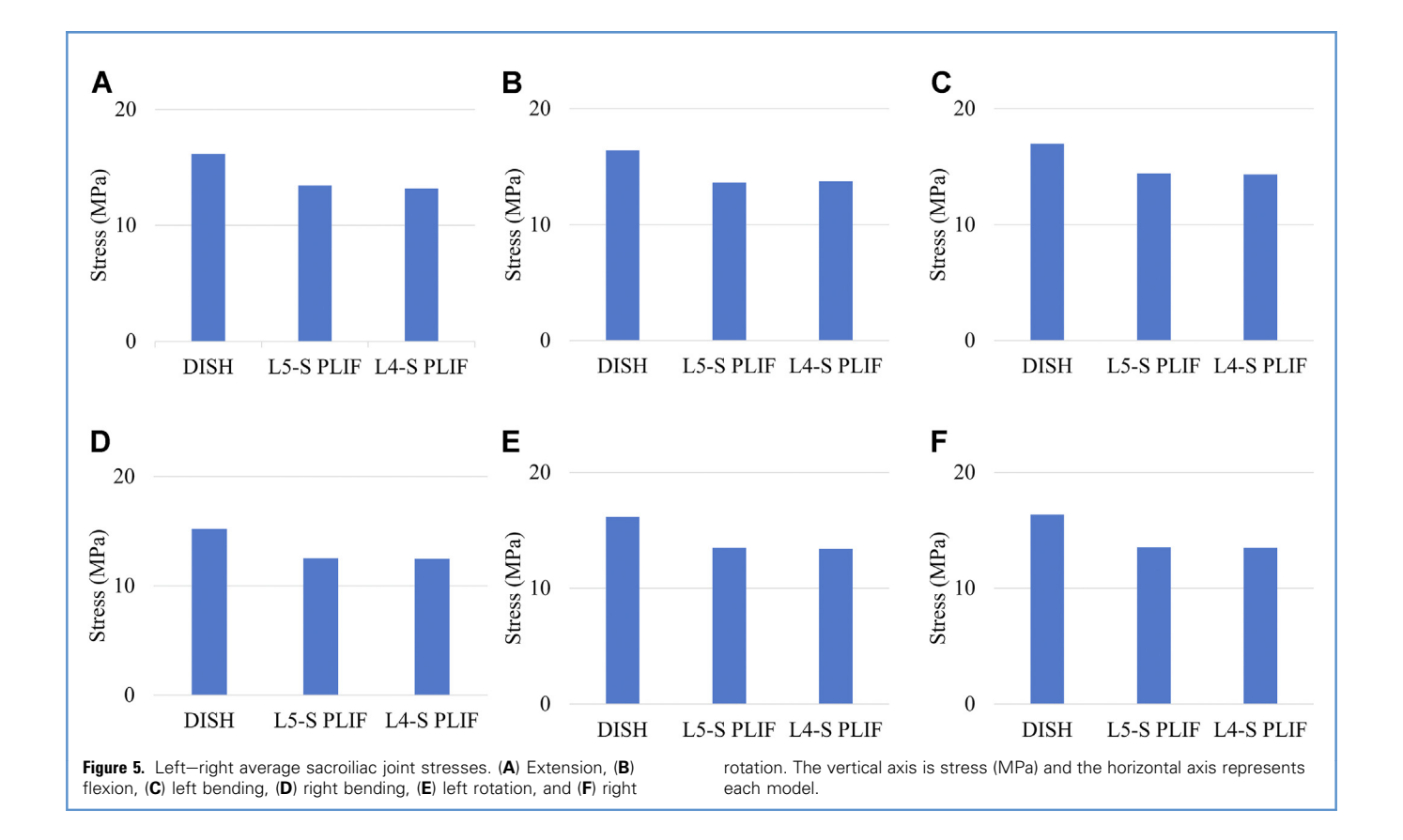
Maximum von Mises stress values on the screws, rods, and cages are shown in **Tables 2** and **3** for L<sub>5</sub>-S PLIF and L<sub>4</sub>-S PLIF. The stress values of screws and rods in the L<sub>4</sub>-S PLIF model was higher than in the L<sub>5</sub>-S PLIF model. The stress values on the L<sub>5</sub>-S cages in the L<sub>5</sub>-S PLIF model were similar or lower than in the L<sub>4</sub>-S PLIF model (**Tables 2** and **3**).

## **DISCUSSION**

In this study, we conducted a 3D FE analysis of PLIF in LSS with DISH. Previous clinical and biomechanical studies have identified issues such as ASD and decreased ROM as a result of DISH and







fixation. Daming et al.<sup>10</sup> reported that PLIF may be used as a treatment option for LSS with DISH when conservative treatment fails. However, because this procedure results in decreased mobility of the spine overall, long-term follow-up is required to fully evaluate the merits and demerits of PLIF. Some studies<sup>9,27</sup> reported the occurrence of ASD and cage retropulsion caused by the mechanical stress on segments of the caudal segment of DISH. Nakajima et al.<sup>27</sup> reported that short fixation for patients

with DISH showed significant development of ASD. Long fixation is recommended to prevent ASD. However, the mechanical events caused by short fixation should be understood. The present analysis agreed with these reports because the L5-S PLIF on LSS with DISH affecting the L1-L4 segments showed increase in stress on the L4-L5 segment; the L4-S fixation did not significantly change the stress on the L5-S cage or the L4-S instrumentation, although the overall L1-L5 ROM decreased.

Motion	Maximum von Mises Stress on Screws Under L5-S PLIF (MPa)	Maximum von Mises Stress on Screws Under L4-S PLIF (MPa)	Maximum von Mises Stress on Rods Under L5-S PLIF (MPa)	Maximum von Mises Stress on Rods Under L4-S PLIF (MPa)
Extension	23	22	184	193
Flexion	24	24	173	184
Left bending	28	46	265	268
Right bending	47	49	428	370
Left rotation	23	27	201	222
Right rotation	23	22	162	164

<b>Table 3.</b> Maximum von Mises Stress Values on the Cage Under L5-S PLIF and L4-S PLIF							
Motion	Maximum von Mises Stress on L5-S Cages Under L5-S PLIF (MPa)	Maximum von Mises Stress on L5-S Cages Under L4-S PLIF (MPa)	Maximum von Mises Stress on L4-S Cages Under L5-S PLIF (MPa)				
Extension	35	36	30				
Flexion	35	36	40				
Left bending	52	48	54				
Right bending	37	28	21				
Left rotation	35	36	31				
Right rotation	36	36	33				

To our best knowledge, a biomechanical analysis of DISH has not been reported, although a previous study<sup>2</sup> indicated that DISH tends to increase stress of the vertebrae and intervertebral disc as a result of reduced flexibility. A study by Sim et al.<sup>28</sup> examined different modes of motion (flexion, extension, right and left lateral bending, and right and left axial rotation) by using L2-S2 spine specimens with L4-L5 PLIF. These results indicated that ROM was reduced with respect to the intact specimens in the PLIF group by 69% in flexion-extension; 73% in lateral bending; and 34% in axial rotation, respectively. The ROM and disc pressure on the adjacent segment of PLIF increased by more than 20% compared with that of the intact specimen in flexion-extension loads. Goto et al.<sup>29</sup> created and compared an L<sub>I</sub>-L<sub>5</sub> FE intact model and an L4-L5 PLIF model; the stress on the adjacent segment of the PLIF model was higher by 117% compared with the intact model. Jiang et al.30 found that the stress on the L3-L4 nucleus pulposus after L4-L5 PLIF increased by 2%, 33%, 3%, and 5% in flexion, extension, lateral bending, and rotation, respectively. Umale et al.31 created a T12-sacrum FE (intact) model and L4-L5 PLIF model and found that ROM of the PLIF model decreased by about 15% and the stress of the cranial and caudal side of fixation level disc pressure increased by more than 10% compared with their intact model. Although previous reports did not consider the length of fixation of PLIF, DISH, SIJ, and hip stresses, PLIF decreased ROM in the whole lumbar and increased adjacent segment disc stresses and segmental ROM in the current study, which agrees with previous reports.

Clinically, Shin et al.<sup>20</sup> reported that the lumbopelvic sagittal imbalance and inadequately restored lumbar lordosis may play a

central role in the development of SIJ pain after PLIF. In this study, we found that there was a decrease in SIJ stresses and no change to hip stress. These results can be attributed to the FE model being created from CT scans of a healthy patient. In the long-term, because the SIJ and hip joint are movable joints in DISH, stress may change after intervertebral fusion or when the deformity progresses gradually. If the sacral slope or pelvic tilt is altered, the SIJ and hip stress may change, although this is out of the scope of the current study.

This study has some limitations. First, it lacks muscle forces that were replaced by follower loads and does not include paraspinal muscles. Second, this model was constructed from CT scans of a young healthy adult and did not consider age-related deformities, bone mineral change, and degenerative changes. The mechanical behavior of the ligaments also changes with age, <sup>21</sup> but that has not been examined in our study. This aspect should be explored in future studies to receive patient-specific and more accurate clinical results. The current study also used only a normal spinopelvic alignment. Our study simulated the immediate postoperative models and did not consider conditions such as union/nonunion between the intervertebral cage and vertebrae and does not fully grasp the long-term biomechanical results of the 4 surgical techniques. Despite these limitations, our study provides valuable insights into DISH and PLIF.

#### **CONCLUSIONS**

The concentration of stress caused by DISH may influence ASD of the nonunited segment in PLIF. Fixation of all the intervertebral segments prevented concentrating stresses. However, because of the long fixation length, stress on the instrumentation cannot be decreased and ROM of the spine was reduced. A short-level lumbar interbody fusion may be recommended to preserve ROM, although it should be used with because it may provoke ASD.

## **CREDIT AUTHORSHIP CONTRIBUTION STATEMENT**

Norihiro Nishida: Conceptualization, Methodology, Formal analysis, Data curation, Writing — original draft. Muzammil Mumtaz: Methodology, Validation, Writing — review & editing. Sudharshan Tripathi: Methodology, Formal analysis, Data curation. Yogesh Kumaran: Writing — review & editing. Amey Kelkar: Methodology, Writing — review & editing. Takashi Sakai: Supervisor. Vijay K. Goel: Supervisor.

#### **REFERENCES**

- Resnick D, Guerra J Jr, Robinson CA, Vint VC. Association of diffuse idiopathic skeletal hyperostosis (DISH) and calcification and ossification of the posterior longitudinal ligament. AJR Am J Roentgenol. 1978;131:1049-1053.
- Nishida N, Jiang F, Ohgi J, et al. Biomechanical analysis of the spine in diffuse idiopathic skeletal hyperostosis: finite element analysis. Appl Sci. 2021;11:8944.
- Kagotani R, Yoshida M, Muraki S, et al. Prevalence of diffuse idiopathic skeletal hyperostosis (DISH) of the whole spine and its association with lumbar spondylosis and knee osteoarthritis: the ROAD study. J Bone Miner Metab. 2015;33:221-229.
- Holton KF, Denard PJ, Yoo JU, Kado DM, Barrett-Connor E, Marshall LM. Diffuse idiopathic skeletal hyperostosis and its relation to back pain among older men: the MrOS Study. Semin Arthritis Rheum. 2011;41:131-138.
- Fujita N. Lumbar spinal canal stenosis from the perspective of locomotive syndrome and metabolic syndrome: a narrative review. Spine Surg Relat Res. 2021;5:61-67.
- Fenton-White HA. Trailblazing: the historical development of the posterior lumbar interbody fusion (PLIF). Spine J. 2021;21:1528-1541.
- Nakajima H, Watanabe S, Honjoh K, Kubota A, Matsumine A. Pathomechanism and prevention of further surgery after posterior decompression for lumbar spinal canal stenosis in patients with

- diffuse idiopathic skeletal hyperostosis. Spine J. 2021;21:955-962.
- Yamada K, Satoh S, Hashizume H, et al. Diffuse idiopathic skeletal hyperostosis is associated with lumbar spinal stenosis requiring surgery. J Bone Miner Metab. 2019;37:118-124.
- Kato S, Terada N, Niwa O, Yamada M. Risk factors affecting cage retropulsion into the spinal canal following posterior lumbar interbody fusion: association with diffuse idiopathic skeletal hyperostosis. Asian Spine J. 2021;15;840-848.
- 10. Chi D, Miyamoto K, Hosoe H, et al. Symptomatic lumbar mobile segment with spinal canal stenosis in a fused spine associated with diffused idiopathic skeletal hyperostosis. Spine J. 2008;8: 1019-1023.
- II. Joukar A, Shah A, Kiapour A, et al. Sex specific sacroiliac joint biomechanics during standing upright: a finite element study. Spine (Phila Pa 1976). 2018;43:E1053-E1060.
- 12. Wu G, Siegler S, Allard P, et al. ISB recommendation on definitions of joint coordinate system of various joints for the reporting of human joint motion-part I: ankle, hip, and spine. International Society of Biomechanics. J Biomech. 2002;35: 543-548.
- Anderson AE, Ellis BJ, Maas SA, Peters CL, Weiss JA. Validation of finite element predictions of cartilage contact pressure in the human hip joint. J Biomech Eng. 2008;130:051008.
- 14. Harris MD, Anderson AE, Henak CR, Ellis BJ, Peters CL, Weiss JA. Finite element prediction of cartilage contact stresses in normal human hips. J Orthop Res. 2012;30:1133-1139.
- Bergmann G, Deuretzbacher G, Heller M, et al. Hip contact forces and gait patterns from routine activities. J Biomech. 2001;34:859-871.
- Goel VK, Grauer JN, Patel T, et al. Effects of charité artificial disc on the implanted and adjacent spinal segments mechanics using a hybrid testing protocol. Spine (Phila Pa 1976). 2005;30: 2755-2764.

- Dalstra M, Huiskes R, van Erning L. Development and validation of a three-dimensional finite element model of the pelvic bone. J Biomech Eng. 1995;117:272-278.
- Momeni Shahraki N, Fatemi A, Goel VK, Agarwal A. On the use of biaxial properties in modeling annulus as a holzapfel-gasser-ogden material. Front Bioeng Biotechnol. 2015;3:69.
- Lindsey DP, Kiapour A, Yerby SA, Goel VK. Sacroiliac joint fusion minimally Affects adjacent lumbar segment motion: afinite element study. Int J Spine Surg. 2015;9:64.
- Shin MH, Ryu KS, Hur JW, Kim JS, Park CK. Comparative study of lumbopelvic sagittal alignment between patients with and without sacroiliac joint pain after lumbar interbody fusion. Spine (Phila Pa 1976). 2013;38:E1334-E1341.
- Mihara A, Nishida N, Jiang F, et al. Tensile test of human lumbar ligamentum flavum: age-related changes of stiffness. Appl Sci. 2021;11:3337.
- Ivanov AA, Kiapour A, Ebraheim NA, Goel V. Lumbar fusion leads to increases in angular motion and stress across sacroiliac joint: a finite element study. Spine (Phila Pa 1976). 2009;34: E162-E169.
- Phillips AT, Pankaj P, Howie CR, Usmani AS, Simpson AH. Finite element modelling of the pelvis: inclusion of muscular and ligamentous boundary conditions. Med Eng Phys. 2007;29: 730-748.
- Butler DL, Guan Y, Kay MD, Cummings JF, Feder SM, Levy MS. Location-dependent variations in the material properties of the anterior cruciate ligament. J Biomech. 1992;25:511-518.
- Joukar A, Chande RD, Carpenter RD, et al. Effects on hip stress following sacroiliac joint fixation: a finite element study. JOR Spine. 2019;2:e1067.
- Kumaran Y, Shah A, Katragadda A, et al. Iatrogenic muscle damage in transforaminal lumbar interbody fusion and adjacent segment degeneration: a comparative finite element analysis of open and minimally invasive surgeries. Eur Spine J. 2021;30:2622-2630.

- Nakajima H, Honjoh K, Watanabe S, Kubota A, Matsumine A. Negative impact of short-level posterior lumbar interbody fusion in patients with diffuse idiopathic skeletal hyperostosis extending to the lumbar segment. J Neurosurg Spine. 2021:1-7.
- 28. Sim HB, Murovic JA, Cho BY, Lim TJ, Park J. Biomechanical comparison of single-level posterior versus transforaminal lumbar interbody fusions with bilateral pedicle screw fixation: segmental stability and the effects on adjacent motion segments. J Neurosurg Spine. 2010;12: 700-708.
- 29. Goto K, Tajima N, Chosa E, et al. Effects of lumbar spinal fusion on the other lumbar intervertebral levels (three-dimensional finite element analysis). J Orthop Sci. 2003;8:577-584.
- Jiang S, Li W. Biomechanical study of proximal adjacent segment degeneration after posterior lumbar interbody fusion and fixation: a finite element analysis. J Orthop Surg Res. 2019;14:135.
- Umale S, Yoganandan N, Baisden JL, Choi H, Kurpad SN. A biomechanical investigation of lumbar interbody fusion techniques. J Mech Behav Biomed Mater. 2022;125:104961.

Conflict of interest statement: The authors declare that the article content was composed in the absence of any commercial or financial relationships that could be construed as a potential conflict of interest.

Received 3 May 2023; accepted 14 May 2023 Citation: World Neurosurg. (2023) 176:e371-e379. https://doi.org/10.1016/j.wneu.2023.05.063

Journal homepage: www.journals.elsevier.com/world-neurosurgery

Available online: www.sciencedirect.com

1878-8750/\$ - see front matter © 2023 Elsevier Inc. All rights reserved.